29th Congress of the International Council of the Aeronautical Sciences
St. Petersburg, Russia; September 7-12, 2014

APPLICATION OF SCALE ADAPTIVE SIMULATION BASED ON K-Ω SST TURBULENCE MODEL

XiangYu Wang, Dong Li
National Key Laboratory of Science and Technology on Aerodynamic Design and Research, Northwestern Polytechnical University, Xi'an 710072, China

Keywords: *Scale Adaptive Simulation, k-ω SST turbulence model, Detached Eddy Simulation, high wave number damping, numerical simulation*

Abstract

Scale Adaptive Simulation (SAS) based on k-ω SST turbulence model is a more and more popular hybrid RANS/LES method in separated flow simulations. We review the basic theory of SST-SAS and present two approaches of improvement for the problem of high wave number damping. Numerical simulations show that the situation of insufficient viscosity in high wave number in the original SST-SAS is well remedied with the combination of the two above, which could further strengthen the grid adaptability compared with Detached Eddy Simulation (DES) and make the turbulent viscosity determined adaptively according to the local flow motion.

1 General Introduction

Separation together with the production and development of vortex motion is a quite common but complex viscous flow phenomenon. In the field of engineering separated flow numerical simulations, URANS (Unsteady RANS) usually produces too large turbulent viscosity resulting from the too large dissipation, masks the details of tiny eddies and finally gets an unphysical simulation, such as the single-vortex shedding under high Reynolds number. However, if LES (Large Eddy Simulations) is adopted to capture the subtle vortex structure, the computational power is a severe limitation because of the fine grid distribution (especially in the boundary layers) and high order physical simulation techniques [1]. Given this, Spalart [2] has firstly put forward a hybrid RANS/LES method called DES (Detached Eddy Simulation) in which the length scale in the SA turbulence model is represented as a controller of wall-distance function. On one hand, flow is still dominated by the original turbulence model under RANS-type gird in the boundary layer, which actually avoids the increase of calculation; on the other hand, the RANS turbulence model is simplified as a Smagrinsky-like sub-grid model in massive separated region or far flow field, which works as LES instead and decreases the turbulent viscosity greatly. Since it was proposed in 1997, DES has already applied in a variety of engineering flow simulations and got a lot of successful results [3].

However it is worth noting that the transition between RANS and LES in DES is explicitly controlled by wall-distance in SA-DES or modelled length scale in SST-DES [4], which means results of DES would be influenced quite strongly by the given grid distribution. A number of numerical tests have shown that blind grid refinement may lead to severe problems such as GIS (Grid Induced Separation) [5] or LLM (Log-Layer Mismatch) [6]. Towards this concern, Menter and his coworkers put forward SAS (Scale Adaptive Simulation) [7] and brought in a new and self-adaptive function named Von Karmam length scale, which could adjust the local turbulent viscosity according to local flow freely and avoid the filter length scale violently confused under some wrong local grid distribution like what usually occurs in DES. This potential method is more and more popular among CFD researchers and a good example is that the famous commercial software Ansys Fluent has involved in it in its turbulence module since version 13 in 2010, and actually CFX adopted it much earlier.

In this study, SAS based on k-ω SST turbulence model is chosen and its working principles are reviewed. Concerning an attracting issue in present SAS, namely high wave number dumping, two remedies are shown and decaying isotropic turbulence and massive separation around cylinder are numerically simulated to test the behaviour of SAS with these remedies.

2 SST-SAS Model Equations

The standard SST-SAS model equations can be written as [8]

$$\frac{\partial \rho k}{\partial t}+\nabla(\rho U k)=P_k-\rho c_\mu k\omega+\nabla\left[\left(\mu+\frac{\mu_t}{\sigma_k}\right)\nabla k\right] \quad (1)$$

$$\frac{\partial \rho\omega}{\partial t}+\nabla\left(\rho U\omega\right)=\alpha\frac{\omega}{k}P_k+\nabla\left[\left(\mu+\frac{\mu_t}{\sigma_\omega}\right)\nabla\omega\right] -\rho\beta\omega^2+\left(1-F_1\right)\frac{2\rho}{\sigma_{\omega 2}}\frac{1}{\omega}\nabla k\nabla\omega+Q_{SAS} \quad (2)$$

Compared with SST turbulence model equations, there is only one extra source term, Q_{SAS}, added in ω equation and the rest remains unchanged. In Menter's paper [9], when local flow becomes separated Q_{SAS} increases so as the production terms in ω equation. That means larger value of ω will be got which leads to larger magnititude of dissipation term in the k equation. As a result, turbulent kinetic energy decreases and high turbulent viscosity is suppressed in separated region, and no doubt it is also helpful to get a clearer vortex structure. In this way how to formulate a reliable and efficient variable working in Q_{SAS} is the core issue. Generalizing the classical boundary layer length scale proposed by Von Karman to arbitrary flow field, Menter formulated a new length scale as

$$L_{vk}=\kappa\left|\frac{\partial U/\partial y}{\partial^2 U/\partial y^2}\right|=\frac{\sqrt{2S_{ij}S_{ij}}}{\sqrt{\left(\nabla^2 u\right)^2+\left(\nabla^2 v\right)^2+\left(\nabla^2 w\right)^2}} \quad (3)$$

On one hand, L_{vk} can cover all the fluctuation scale in the inertial sub-region, which is actually the original meaning of L_{vk} working as Von Karman length scale; on the other hand, it is self-adjusted all the time in unsteady regions according to the previous known flow motion. Compared with DES, the self-adaption of length scale means not only the accurate flow prediction in boundary layer but also the unnecessary of the explicit chosen interface between RANS and LES [10], which is totally dependent on the grid distribution in DES. In other words, it is L_{vk} that divides the whole field into RANS region (Q_{SAS} =0) or SAS region (Q_{SAS} >0). Finally the formulation of Q_{SAS} reads

$$L=\sqrt{k}/\left(c_\mu^{1/4}\cdot\omega\right) \quad (4)$$

$$Q_{SAS}=\max\left[\begin{array}{l}\rho\zeta_2\kappa S^2\left(\dfrac{L}{L_{vk}}\right)^2- \\ C\cdot\dfrac{2\rho k}{\sigma_\phi}\max\left(\dfrac{\left|\nabla\omega\right|^2}{\omega^2},\dfrac{\left|\nabla k\right|^2}{k^2}\right),0\end{array}\right] \quad (5)$$

Where L is the modelled stress length scale as what it is in SST-DES.

3 Remedies for High Wave Number Damping

However, the numerical simulation under SST-SAS introduced above is usually not stable, which is due to the problem of high wave number damping (HWN) [10]. Actually L_{vk} adopted in SAS is aimed to symbolize the smallest eddy scales, and produce turbulent viscosity small enough accordingly to allow the formation of even smaller eddies until the grid limit is reached and no smaller eddies would be formed afterwards. That is just an ideal situation. Unfortunately there is no self-adjusted mechanism involved in original SAS to help get the information about the cut-off limitation. That means when it comes into cut-off wave number length scales, the eddy that translates from big to small may exceed the limitation of grid resolution, and the kinetic energy cannot go on translating and finally accumulate at the high wave number, for the continuously produced turbulent viscosity together with so small dissipation (L_{vk} is very small and Q_{SAS} is very large accordingly). Moreover, when a mesh has been given, the higher Reynolds number for computation is, the lower gird resolution and the severer unbalance of viscosity production and dissipation are. It can worsen the simulation stability directly and it is quite necessary to add some remedies to increase the eddy dissipation in high wave number and limit the minimum of turbulent viscosity.

Balancing the production and dissipation term in turbulence model equations is a routine way for some derivation and thus when both source terms in k and ω equations are set to zero, following relationships can be got

$$P_k - \rho c_\mu k\omega = 0 \tag{6}$$

$$\alpha \frac{\omega}{k} P_k - \rho\beta\omega^2 + \rho\zeta_2 \kappa S^2 \left(\frac{L}{L_{vk}}\right)^2 = 0 \tag{7}$$

Concerning $\mu_t = k/\omega$ and $P_k = \mu_t S^2$ the two equations above can be simplified as

$$\mu_t^{eq} = \rho\left(\left(\beta / c_\mu - \alpha\right) / \left(\kappa\zeta_2\right)\right) L_{vk}^2 S \tag{8}$$

Obviously the formulation of turbulent viscosity in Eq. (8) is very similar with that in Smagrinsky sub-grid model equation which reads

$$\mu_t^{LES} = \rho\left(C_s \cdot \Delta\right)^2 S \tag{9}$$

Therefore, when $\mu_t^{eq} < \mu_t^{LES}$ Eq. (9) can be used as a remedy and final formulation for L_{vk} is

$$L_{vk} = \max\left(\kappa S / \left|\nabla^2 U\right|, C_s \sqrt{\kappa\zeta_2 / \left(\left(\beta / c_\mu\right) - \alpha\right)} \cdot \Delta\right) \tag{10}$$

Actually Eq. (10) is also the remedy in Menter's latest work [9] about SST-SAS. Unlike DES which adopts either RANS or LES in fixed region as the grid is fixed, it is possible that SAS with this remedy may degenerate into a potential DES-like method overall, since the the new length scale itself is very sensitive and the ubiquitous vortex motion, including production, development, transition, dissipation and vanishment of eddies, means this remedy may also reach throughout the entire field all the time. Concerning k equation itself does not resolve local length scale and only the change of ω indirectly affects the dissipation term of k equation, the formulation of k equation in DES can be taken as reference and finally we can get

$$\frac{\partial \rho k}{\partial t} + \nabla \bullet (\rho U k) = P_k - \frac{\rho k^{3/2}}{l_k} + \nabla \bullet \left[\left(\mu + \frac{\mu_t}{\sigma_k}\right)\nabla k\right] \tag{11}$$

$$l_k = \min\left(k^{1/2} / c_\mu \omega, \kappa S / \left|\nabla^2 U\right|\right) \tag{12}$$

Namely the new length scale L_{vk} is also adopted instead of original one $C_{DES}d$. When the value of L_{vk} is small, the magnititude of dissipation term in k equation will be quite large which can directly suppress the accumulation in high wave number. That is to say L_{vk} works as a parameter to scale local kinetic energy and this new remedy is independent on the grid distribution and anymore, without adding other defined variables. In particular, although L_{vk} has been coupled in k equation and functions as a common length scale for both k and ω equation to detect local turbulence, SAS seems still sensitive to flow changes without any information about grid because of its weak dissipation. Actually the following tests show that the combination of both these two remedies is better than either one.

4 Test Cases

4.1 Decaying Homogenous Isotropic Turbulence

In this paper simulation of Decaying Homogenous Isotropic Turbulence (DHIT) under the computational conditions of Samtaney [11, 12] is chosen as the test for the damping characteristics of SAS. Using an equidistant grid of 128^3 volumes, the recommended parameter C_s=0.11 from Menter is adopted firstly. Fig.1 shows the flow structures and the color of the structures is the Von karmam turbulent length scale, L_{vk}, divided by the grid spacing $2\pi/128$. That the ratio is of the order of 0.18 means SAS is returning a length scale much smaller than the domain size. Moreover, it is clear that the combination of the two corrections (L_{vk} limiter and turbulence energy localization) above has remedied the behavior of insufficient damping effectively from Fig.2 (a). Different from the Von Karmam length scale, which is totally dependent on local flow, C_s in the L_{vk} limiter is an independent parameter that should be calibrated. To a given mesh, a larger C_s means smaller cutting wave number k_c because of the inverse proportional relationship $k_c \sim \pi/C_s\boldsymbol{\Delta}$, which further leads to the decrease of resolved scale and the increase of subgrid viscosity and suppress of high wave turbulent energy accumulation. Given this, next we present four solutions to test influence of different values of C_s.

Solver 1: SST-SAS + L_{vk} limiter (C_s=0.05)
Solver 2: SST-SAS + L_{vk} limiter (C_s=0.5)
Solver 3: SST-SAS + L_{vk} limiter (C_s=0.05) + turbulence energy localization
Solver 4: SST-SAS + L_{vk} limiter (C_s=0.5) + turbulence energy localization

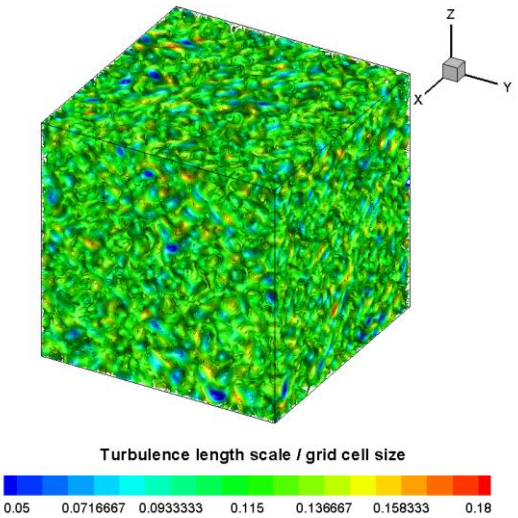

Fig.1 Resolved structures in DHIT case for SST-SAS model (Grid 128×128×128)

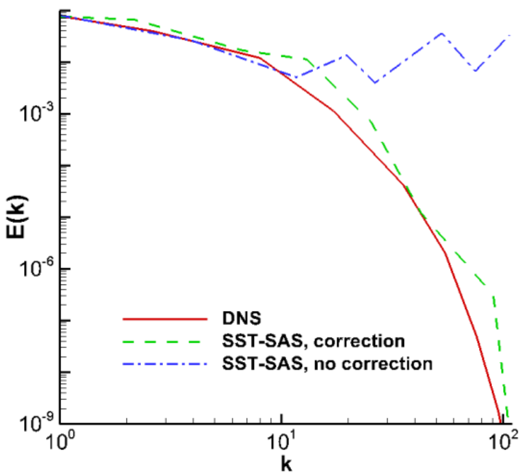

(a)

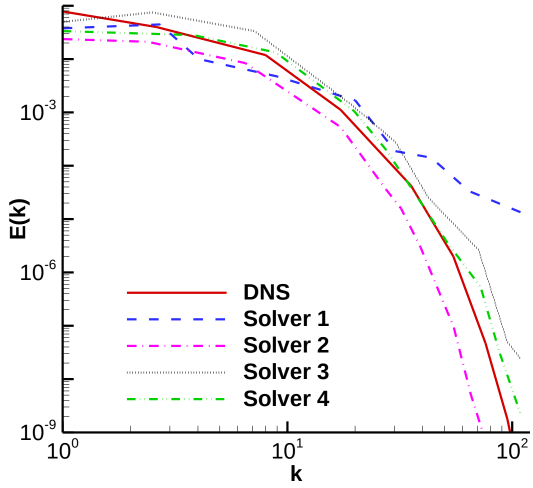

(b)

Fig.2 Spectra of the resolved kinetic energy (t=1.5)

As what shown in Fig.2 (b), relative error in Solver 1 and 2 are greater than the other two and their respective trend profiles are consistent with the analyses above. It proves that unsuitable C_S may play a negative role in this remedy, which is similar as the influence of C_{DES} in DES. Conversely, Solver 3 and 4 are obviously less influenced by the different values of C_s. That means the new remedy, turbulence energy localization, can effectively improve robustness of L_{vk} limiter.

4.2 Massive Separation around Circle Cylinder

This case [12] is set up to compare the different simulation results between SST-SAS and SST-DES and keep on testing the effect of remedies above in SST-SAS at the same time. The circle cylinder model has a low Mach number of *Ma*=0.2 and a high Reynolds number of $Re=1.8\times10^5$. The far-field domain boundary is approximately 20*D* (*D* means the diameter of the circle cylinder) away from the wall. There are 200×180 points distributed in an O-type topology in the streamwise slice, and the 3D mesh is an extrusion in the spanwise direction of this 2*D* mesh, with 40 elements uniformly distributed over a spanwise length of 2*D*. The first layer of mesh in the wall-normal direction maintains y^+=1.5, as the order of $1\times10^{-5}D$. Noting that here SAS involves both the remedies above, and the parameter CDES in SST-DES reads

$$C_{DES} = F_1 C_{DES}^{k-\omega} + \left(1 - F_1\right) C_{DES}^{k-\varepsilon}$$
$$C_{DES}^{k-\omega} = 0.78, C_{DES}^{k-\varepsilon} = 0.61 \tag{13}$$

where F_1 is the shielding function in SST turbulence model itself. Fig.2 and 3 show the pressure distributions on the surface and the vorticity magnitude in the mid streamwise slice.

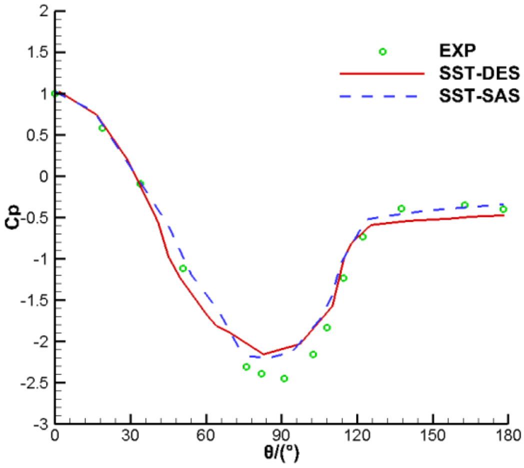

Fig.2 Pressure distribution (standard mesh)

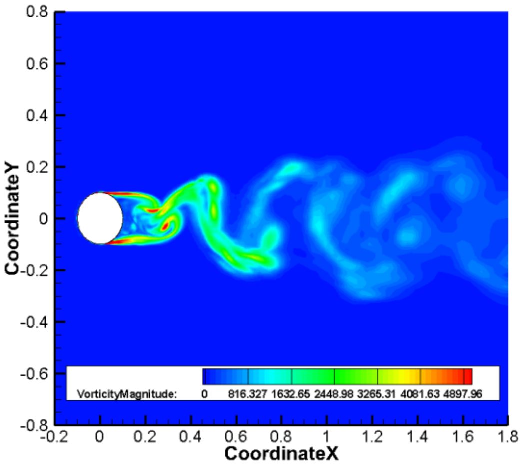

Fig.3 Vorticity magnitude (SAS, standard mesh)

Obviously SAS with remedies for high wave damping works well, as well as SST-DES. That may result from the suitable mesh distribution recommended in reference [13]. Then, a poor mesh for SST-DES is chosen purposely to further investigate the difference between these two methods. The new mesh has a less gird number, 200×140 in streamwise slice and its y^+ equals to 0.1 rather than previous 1.5, which means the points distribution in wall-normal direction is unreasonablely finer near the surface and coarser far away. The simulation results are shown in Fig. 4 and 5. Although we also get vortex shedding from SST-DES, the small-scale vortex are dissipated seriously because of the too large subgrid viscosity controlled by the poor mesh. As a comparison SAS still maintain similar result that the downstream vortex has fully developed. Noting that *Cs* and C_{DES} adopted here are same with what used under the standard mesh above. Noting actually if we adjust the C_{DES} to some degree to decrease the mesh-caused viscosity artificially, SST-DES may also simulate better. Of course this does not conflict with the conclusion that SAS is more adaptable and stable.

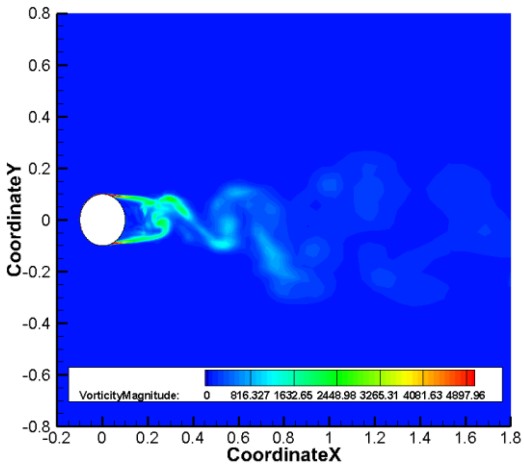

(a) SST-DES

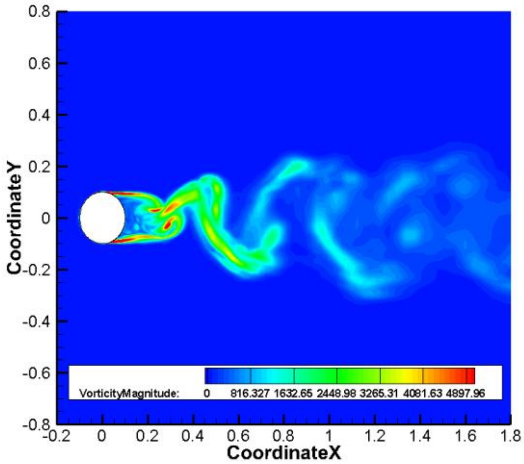

(b) SST-SAS

Fig.4 Vorticity magnitude (poor mesh)

Fig.5 shows the pressure distributions under the poor mesh, in which SST-SAS-1 means only L_{vk} limiter is adopted in that case and SST-SAS-2 involves both the two remedies. On one hand, unreasonable mesh distribution leads to a potential grid induced separation in SST-DES, and negative pressure peak is ahead of the experiment results. However, SST-SAS-2 gets a totally similar simulation with the above test case under standard mesh, which adds credence that SST-SAS is more robust. On the other hand, comparing the results in SST-SAS-1 and 2, single L_{vk} limiter remedy cannot fundamentally prevent the trend that SST-SAS degenerate to SST-DES under some poor mesh. At the same time, instant detail monitor shows that about 8% grid cells are still remedied by L_{vk} limiter. Taking into account all the factors above, remedy of turbulence energy localization is a generation of scale adaptive simulation from only k equation to both k and ω equations, and plays a decisive role to improve the mesh adaptation by combining the whole SST turbulence model with one parameter, Von Karman length scale. While not bringing in any information for mesh resolving, SAS itself with only turbulence energy localization cannot solve the problem of high wave number damping completely. That is why we still need L_{vk} limiter to force the minimum of viscosity explicitly. Maybe there are few cell numbers controlled by L_{vk} limiter, however, the influence of it for a stable simulation is great. A good example is that if we choose a SST-SAS-3 which only involves the remedy of turbulence energy localization in this test case, it could be easily found the simulation would diverge at the end.

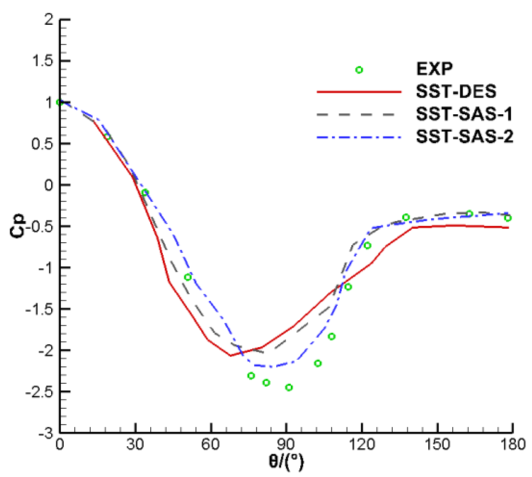

Fig.5 Pressure distribution (poor mesh)

5 Conclusions

A new and popular hybrid RANS/LES method, SST-SAS, is basically reviewed. Concerning the issue of high wave number damping we compare two main remedies, L_{vk} limiter and turbulence energy localization. Specifically turbulence energy localization integrates the whole k-ω turbulence model by Von Karman length scale and improves the grid adaptation, increases the high wave number damping entirely. Although L_{vk} limiter keeps the inherent defect of DES to some degree, it remedies the local insufficient viscosity forcedly and is great helpful for a stable simulation. The complementary relationship between these two remedies is tested by two typical cases, decaying isotropic turbulence and massive separation around circle cylinder. With the remedies both, SST-SAS shows more grid adaptive than original SST-DES and even if under some poor grid distribution, SST-SAS can also get satisfactory simulations.

References

[1] Durrani N, Qin N. Behaviour of Detached-Eddy Simulations for mild trailing-edge separation. *Journal of Aircraft*, Vol. 48, No.1, pp 193-202, 2011

[2] Spalart P R. Strategies for Turbulence Modeling and Simulations. *International Journal of Heat fluid flow*. Vol. 21, pp 252-263, 2000

[3] Spalart P R. Detached-Eddy Simulation. *Annual Review of Fluid Mechanics*. Vol. 41, pp 181-202, 2009

[4] Strelets M. Detached eddy simulations of massively separated flows. *AIAA Paper*, 2001-0879, 2001

[5] Spalart P R. Young-person's guide to detached-eddy simulation grids. *NASA-TM*, 2001-211032, 2001

[6] Shur M L, Spalart P R, Strelets A, Travin A. A rapid and accurate switch from RANS to LES in boundary layers using an overlap region. *Turbulence and combustion*, Vol. 86, pp 179-206, 2011

[7] Menter F R, Kuntz M, Bender R. A scale-adaptive simulation model for turbulent flow predictions. *AIAA Paper*, 2003-0767, 2003

[8] Menter F R, Egorov Y. A scale-adaptive simulation model using two-equation models. *AIAA Paper*, 2005-1095, 2005

[9] Egorov Y, Menter F R. Development and Application of SST-SAS Turbulence Model in the DESIDER Project. *2007 Symposium on Hybrid RANS-LES Methods*, Corfu, NNFM 97, pp 261–270, 2008

[10] Menter F R, Egorov Y. The Scale-Adaptive Simulation Method for Unsteady Turbulent Flow Predictions. *Flow Turbulence Combust*, Vol 85, pp 113-138, 2010

[11] Samtaney R, Pullin D I, Kosovi B. Direct numerical simulation of decaying compressible turbulence and shocklet statistics. *Physics of Fluids*, Vol.13, No. 5, pp 1415-1430, 2001
[12] Li X L, Fu D, Ma Y. Direct numerical simulation of compressible isotropic turbulence. *Science in China A*, Vol. 45, No. 11, pp 1452-1460, 2002
[13] Roshko A. Experiments on the flow past a circular cylinder at very high Reynolds number. *Journal of fluid Mechanics*. Vol. 10, No. 3, pp 345-356, 1961

Contact Author Email Address

Mail to: xiangyu.wang@mail.nwpu.edu.cn; ldgh@nwpu.edu.cn

Copyright Statement